# ATMOSPHERIC NEUTRINO OSCILLATION RESULTS WITH MACRO AT GRAN SASSO LABORATORY

M. SPINETTI
(for the MACRO collaboration)
*INFN Laboratori Nazionali di Frascati P.O. Box 13, I–00044 Frascati ITALY*
E–mail: spinetti@lnf.infn.it

## Abstract

We present updated results of the measurement of the atmospheric neutrino flux with the MACRO detector at Gran Sasso, using three data sets spread in a large energy range. In the high energy range, the upgoing throughgoing muon data set is in favor of $\nu_\mu \to \nu_\tau$ oscillation hypothesis with a probability of 36.6% against the 0.36% for the no oscillation hypothesis.

In the low energy range, the two data set are also in favor to the oscillation hypothesis showing a large deficit for IU events and a reduced deficit for US+ID events, since only the US events ( ≈50% ) are expected to oscillate

Assuming a $\nu_\mu \to \nu_\tau$ oscillation scheme, the results suggest a large range of the parameter values centered around $\Delta m^2 = 0.0025$ eV$^2$, $\sin^2 2\theta = 1$.

PACS.: 96.40.Tv

## 1. Introduction

The past observations of Kamiokande[1], IMB[2] and Soudan 2 [3] on the anomaly in the atmospheric neutrino ratio of contained muon neutrino to electron neutrino interactions is now well confirmed. The recent results obtained by SuperKamiokande[4] with much larger statistics have well established the anomaly which finds an explanation in the scenario of $\nu_\mu \to \nu_\tau$ oscillation with a $\Delta m^2$ in the range of a few times $10^{-3}$ eV$^2$ and maximal mixing.

The effects of neutrino oscillations have to appear in higher energy ranges as well in the low energy ranges according to the relevant oscillation parameter L/E. In the high energy region, from a few GeV up to a few TeV, the flux of atmospheric muon neutrinos can be inferred from measurements of upward throughgoing muons. Several results have been obtained in the past by IMB[5], Kamiokande[6], Macro[7] and recently by Macro [8] and SuperKamiokande[9] with larger statistics.

As a consequence of the oscillations, the flux of upward throughgoing muons should be affected both in the absolute number of events and in the shape of the zenith angle distribution, with relatively fewer observed events near the vertical than near the horizontal due to the longer path length of neutrinos from production to observation.

Furthermore, in the few GeV energy region, the flux of atmospheric muon neutrinos can be studied looking at muons produced inside the detector and also looking at muons externally produced and stopping inside it. If the atmospheric neutrino anomalies are the result of neutrino oscillations, it is expected a reduction in the flux of upward-going low-energy atmospheric neutrinos of about a factor of two, but without any distortion in the shape of the angular distribution. Results for this kind of events have already been reported by Macro [10,11].

Here an update of all the results obtained by MACRO is presented.


## 2. Neutrino events in the Macro detector

The MACRO detector [12] is located in the Gran Sasso Laboratory, with a minimum rock overburden of 3150 hg/cm$^2$. It is a large rectangular box (76.6x12x9.3m$^3$) divided longitudinally in six similar supermodules and vertically in a lower (4.8 m high) and an upper part (4.5 m high). Active elements are streamer tubes used for tracking and liquid scintillation counters used for the time measurement. The lower part is filled with trays of crushed rock absorber alternating with streamer tube planes, while the upper part is open and contain the electronics racks. The intrinsic angular resolution for muons typically ranges from 0.2° to 1° depending on the track length. This resolution is lower than the angular spread due to multiple scattering of muons in the rock. The scintillator system consists of three layers of horizontal counters, with vertical counters along the sides of the detector. The time and position resolutions for muons in a scintillation counter are about 0.5 ns and 11 cm, respectively. Thanks to its large area, fine tracking granularity and electronics symmetry with respect to upgoing and downgoing flight direction, the MACRO detector is a proper tool for the study of upward-traveling muons, generated by external interactions. Its mass permits also to collect a statistically significant number of neutrino events due to internal interactions.

Figure 1A shows a schematic plot of three different event topologies of neutrino events analyzed in this work. The requirements for reconstructing a track select mostly muons generated in $\nu_\mu$ Charged Current interactions.

Figure 1B shows the parent neutrino energy distribution for the different event topologies. The three event topologies are the following:

1. Up-Throughgoing muons – These tracks come from interactions in the rock below MACRO and cross the whole detector ($E_\mu > 1$ GeV). The time-of-flight information provided by scintillation counters permits to know the muon flight direction. The convention is that $1/\beta = -1$ is for upgoing muons. The data have been collected, since March 1989, with three different detector configurations (4.6 years of total equivalent live time ). The median energy is around 50 GeV.

2. Internal muons (IU) – These partially contained events come from $\nu_\mu$ interactions inside the massive lower part of the detector. Also in this case the time-of-flight method is applied to identify the events. Hence only the data collected with the full detector configuration can be used ( total live time 4.1 years ) have been used in this analysis. About 11% of events are estimated to be induced by $\nu_e$ interactions and NC. The median energy is around 4 GeV

3. Upgoing Stopping and Internal Downgoing (US+ID) – This sample is composed by two subsamples: interactions in the rock below MACRO with an upgoing track stopping in the detector (US) and interactions inside the massive lower part of the detector with a downgoing track (ID). These events are identified by means of topological criteria. The lack of time information prevents to distinguish the two subsamples which are expected to be almost equally populated if neutrinos do not oscillate. About 13% of events are estimated to be induced by $\nu_e$ interactions and NC. The median energy is around 3 GeV
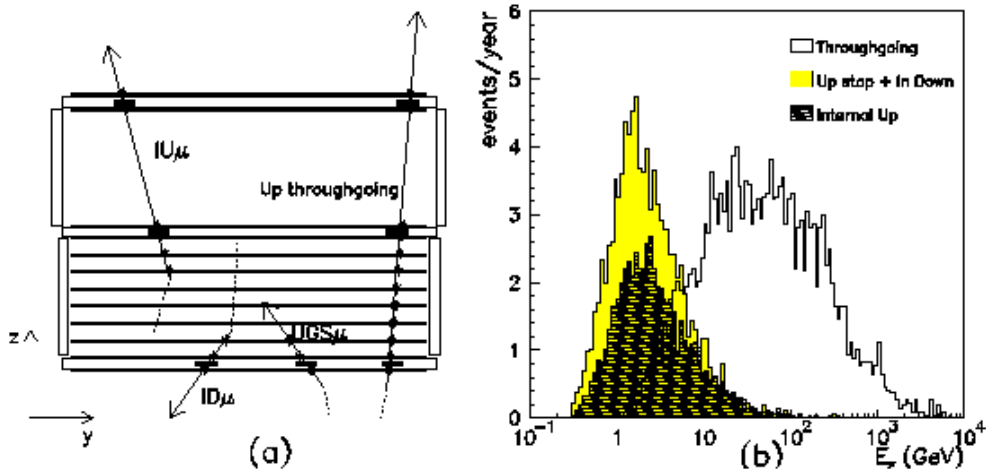


Fig. 1. **a)** Sketch of different event topologies induced by neutrino interaction in or around MACRO. IUμ= Internal Upgoing muons; IDμ= Internal Downgoing muons; UGSμ= Upgoing Stopping muons; Up-throughgoing = Upward throughgoing muons. In the figure, the stars represent the streamer tube hits, and the black boxes the scintillator hits. The *T.o.F.* of the particle can be measured for the IUμ and Up-throughgoing events. **b)** Parent neutrino energy distribution for the three $\nu_\mu$ samples.

## 3. Upward Throughgoing Muons

Several cuts are imposed to remove backgrounds caused by radioactivity or showering events which may result in bad time reconstruction. The most important cut requires that the position of a muon hit in each scintillator as determined from the timing within the two counter ends agrees within 70 cm with the position indicated by the streamer tube track. When a muon hits 3 scintillator layers (about 50% of the tracks), there is redundancy in the time measurement and $1/\beta$ is calculated from a linear fit of the times as a function of the path length. Tracks with a poor

fit are rejected. Other minor cuts are applied for the tracks with only two scintillator layer hits.

It has been observed that downgoing muons which pass near or through MACRO may produce low energy, upgoing particles. These could appear to be neutrino-induced upward throughgoing muons if the downgoing muon misses the detector [13]. In order to reduce this background, a cut is imposed requiring that each upgoing muon must cross at least 200 g/cm$^2$ of material in the bottom half of the detector. Finally, a large number of nearly horizontal (cos θ > -0.1 ), but upgoing muons have been observed coming from azimuth angles corresponding to a cliff in the mountain where the overburden is insufficient to remove nearly horizontal, downgoing muons which have scattered in the mountain and appear as upgoing. This region is excluded from both data and Montecarlo simulation.
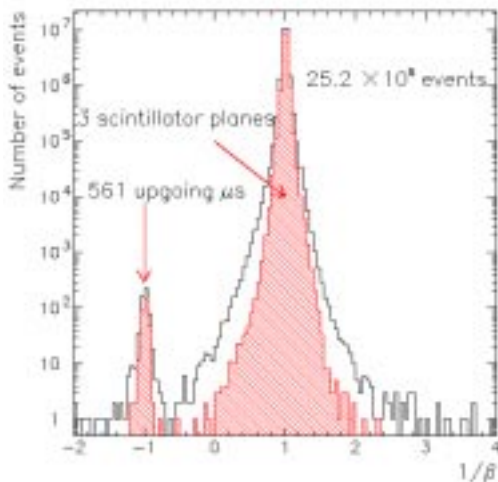


Fig. 2. Distribution of 1/β for the full detector data set. A clear peak of upgoing muons is evident centered at 1/β =-1. The widths of the distributions for upgoing and downgoing muons are consistent. The shaded part of the distribution is for the subset of events where three scintillator layers were hit.

Figure 2 shows the 1/β distribution for the throughgoing data taken with the full detector running. A clear peak of upgoing muons is evident centered on 1/β =-1. There are 561 events in the range -1.25 <1/β < -0.75 defined as upgoing muons for this data set. Combining these data with the previously published data [7] for a total of 642 upgoing events. Based on events outside the upgoing muon peak, 12.5±6 background events are estimated to be subtracted to the total data set. In addition, 10.5±4 events are estimated as resulting from upgoing charged particles produced by downgoing muons in the rock near MACRO. Finally, 12±4 events are estimated as resulting from interactions of neutrinos in the very bottom layer of MACRO scintillators, events which are not included in flux calculations. Hence, removing the backgrounds, the observed number of up-throughgoing muons integrated over all zenith angles is 607.

In the up-throughgoing muon simulation, the neutrino flux computed by the Bartol group have been used[14]; it is affected by a systematic uncertainty of ±14%, taking into account the agreement with measurements of the muon flux in the atmosphere. The cross-sections for the neutrino interactions have been calculated using the GRV94 [15] parton distributions set, which varies by +1% respect to the Morfin and Tung parton distribution used in the past. It is estimated a systematic error of 9 % on the upgoing muon flux due to uncertainties in the cross section including low energy effects [16]. The propagation of muons to the detector has been

done using the energy loss calculation [17] for standard rock. The total theoretical uncertainty on the expected muon flux, adding the errors from neutrino flux, cross-section and muon propagation in quadrature, is ±17%. This theoretical error in the prediction is mainly a scale error that doesn't change the shape of the angular distribution. The detector and the triggers are fully reproduced in a Geant based Montecarlo program. Real and simulated data are analyzed with the same analysis chain. Particular care has been taken to minimize the systematic uncertainty in the detector acceptance simulation. Different acceptance calculations, including separate electronic and data acquisition systems, have been compared. Four different analysis have been performed getting the same results. Furthermore comparison between upgoing and downgoing data, trigger and streamer tube efficiency, background subtraction, effect of analysis cuts have been in detail studied.
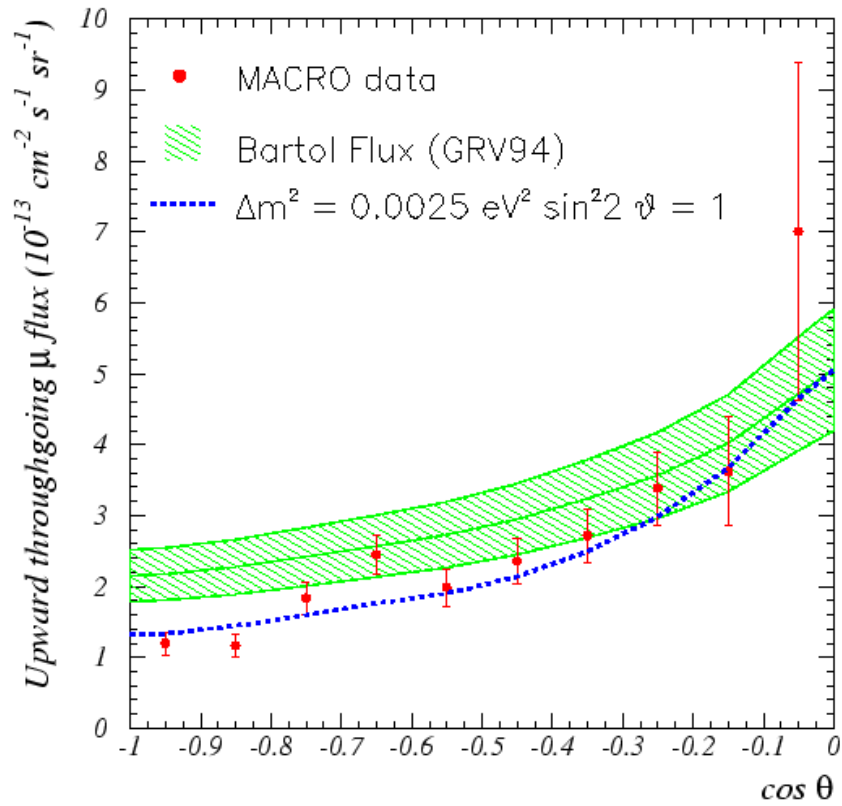


Fig. 3. Zenith distribution of flux of upward throughgoing muons with energy greater than 1 GeV for data and Montecarlo for the combined MACRO data. The shaded region shows the expectation for no oscillations and includes the 17\% uncertainty in the expectation. The lower line shows the prediction for an oscillated flux with $\sin^2 2\theta = 1$ and $\Delta m^2 = 0.0025$ eV$^2$.

The number of events expected integrated over all zenith angles is 825, giving a value for the ratio R of the observed number of events to the expectation of:

$$R = 0.74 \pm 0.031_{stat} \pm 0.044_{sys} \pm 0.12_{theor}.$$

Figure 3 shows the zenith angle distribution of the measured flux of upgoing muons with energy greater than 1 GeV for all MACRO data compared to the Montecarlo expectation for no oscillations and with a $\nu_\mu \rightarrow \nu_\tau$ oscillated flux with $\sin^2 2\theta = 1$ and $\Delta m^2 = 0.0025$eV$^2$ (dashed line).

The shape of the angular distribution has been tested with the hypothesis of no oscillation excluding the last bin near the horizontal and normalizing data and predictions.

The $\chi^2$ is 22.9 which, for 8 degrees of freedom, means a probability of 0.35 % for a shape at least this different from the expectation. Moreover, considering a $\nu_\mu \rightarrow \nu_\tau$ oscillations, the best $\chi^2$ in the physical region of the oscillation parameters is 12.5 for $\Delta m^2 = 0.0025$ eV$^2$ and $\sin^2 2\theta = 1$ (the best $\chi^2$ is 10.6 for an unphysical value of $\sin^2 2\theta = 1.5$).
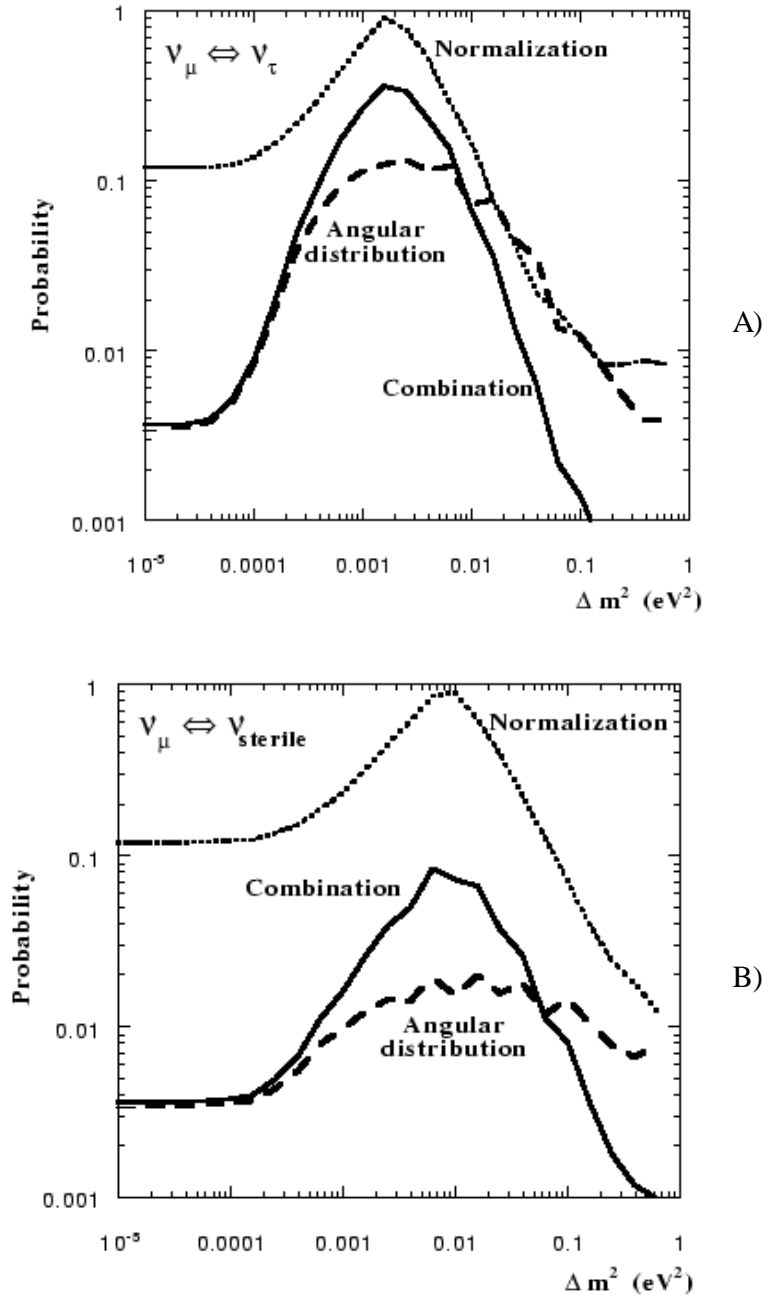


Fig. 4. Probabilities for maximum mixing and oscillations $\nu_\mu \rightarrow \nu_\tau$ A), or oscillations $\nu_\mu \rightarrow$ sterile neutrino B). The 3 lines corresponds to the probability from the total number of events (dotted line), the probability from the chi-square of the angular distribution with data and prediction normalized (dashed line) and to the combination of the two independent probabilities (continuos line).
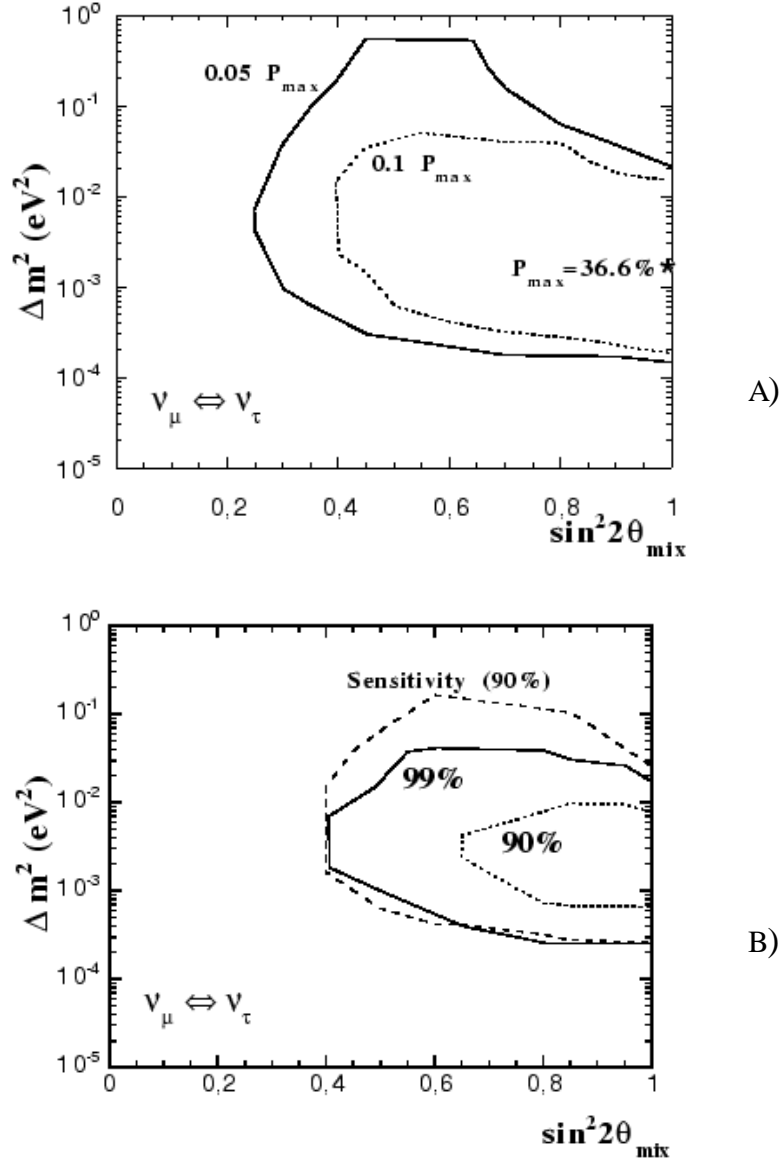
Fig. 5A). Probability contours for oscillation parameters for $\nu_\mu \to \nu_\tau$ oscillations based on the combined probabilities of zenith shape and number of events tests. The best probability in the physical region is 36.6% and iso-probability contours are shown for 10% and 5% of this value (i.e. 3.6% and 1.8%).

B) Confidence regions at the 90% and 99% levels calculated according to Feldman and Cousins [20]. Since the best probability is outside the physical region the confidence interval regions are smaller than the ones expected from the sensitivity of the experiment.

To test the oscillation hypothesis, it is calculated the independent probability for obtaining the number of events observed and the angular distribution for various oscillation parameters. They are reported for $\sin^2 2\theta = 1$ in Figure 4A) for $\nu_\mu \to \nu_\tau$ oscillations. The combined probability is also reported.

It is notable that the value of $\Delta m^2$ suggested from the shape of the angular distribution is close to the value necessary in order to obtain the observed reduction in the total number of events in the hypothesis of maximum mixing.

Figure 4B) shows the same quantities for sterile neutrinos oscillations [18,19].

Figure 5A) shows probability contours for oscillation parameters. The maximum of the probability is 36.6% for oscillations $\nu_\mu \to \nu_\tau$. The best probability for oscillations into sterile neutrino is 8.4 %. The probability for no oscillation is 0.36 %.

Figure 5B) shows the confidence regions at the 90 % and 99 % confidence levels applying the Feldman and Cousins method [20]. The sensitivity of the experiment is also plotted, being the 90 % contour which would result from the preceding method when the data are equal to the Montecarlo prediction at the best fit point.

## 4. Internal Upgoing muons (IU)

The identification of IU events is based both on topological criteria and T.o.F. measurements. The basic requirement is the presence of at least two scintillator clusters in the upper part of the apparatus matching a streamer tube track reconstructed in space. This request is similar to that applied to the up-throughgoing events.

For IU candidates, the track starting point must be inside the apparatus. To reject fake semicontained events entering from a detector crack, the extrapolation of the track in the lower part of the detector must cross and not fire at least three streamer tube planes and one scintillation counter.

The above conditions, tuned on the Montecarlo simulated events, account for detector inefficiencies and reduce the contribution from upward throughgoing muons which mimic semicontained muons to less than $\approx 1\%$. The measured $1/\beta$ distribution is shown in Fig. 6.
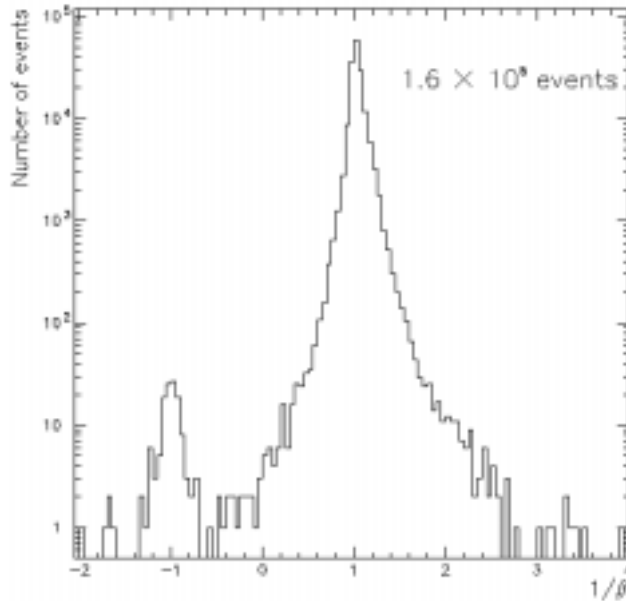


Fig. 6. The $1/\beta$ distribution of the detected IU events (dashed area) after all cuts and the final check of vertex containment. The remaining $1.6 \times 10^5$ events around $1/\beta = 1$ are downgoing atmospheric stopping muons.

After the subtraction of 5 events, due to an uncorrelated background, 116 events are classified as IU events.

The expected rates were evaluated with a full Montecarlo simulation. The events are mainly due to $\nu_\mu$CC, with a contribution from NC and $\nu_e$ of 11%. The neutrinos were allowed to

interact in a volume of rock containing the experimental Hall B and the detector. The rock mass in the generation volume is 170 kton, while the MACRO mass is 5.3 kton. The atmospheric $\nu$ flux of the Bartol group [14] has been used and the cross-sections for the neutrino interactions have been calculated using the GRV94 [15] parton distributions and including low energy effects [16]. The total theoretical uncertainty on the expected rates at these energies is about 25%.

The detector response has been fully simulated using a Geant based Montecarlo as for up-throughgoing events. It accounts for analysis algorithm efficiency, data taking conditions, acceptance and mass of the detector. The systematic error on the data, arising from the simulation of detector response, is about 10%.

The expected IU events is 202, while the observed number of events is 116. So the ratio R of the observed number of events to the expectation becomes:

$$R=0.57\pm0.05_{stat}\pm0.06_{syst}\pm0.14_{theor}.$$

The zenith angle distribution is shown in Fig. 7 left: it shows a uniform deficit of the measured number of events over the whole angular distribution with respect to the predictions based on the absence of neutrino oscillations.
Including the neutrino oscillation effects with the parameters measured with the up-throughgoing muons ($\Delta m^2=0.0025$ eV$^2$ and $\sin^2 2\theta = 1$), the expected number of events becomes 118 well in agreement with the measured one. Moreover also the angular distribution is well in agreement with the measured one (see dashed line in Fig. 7 left).
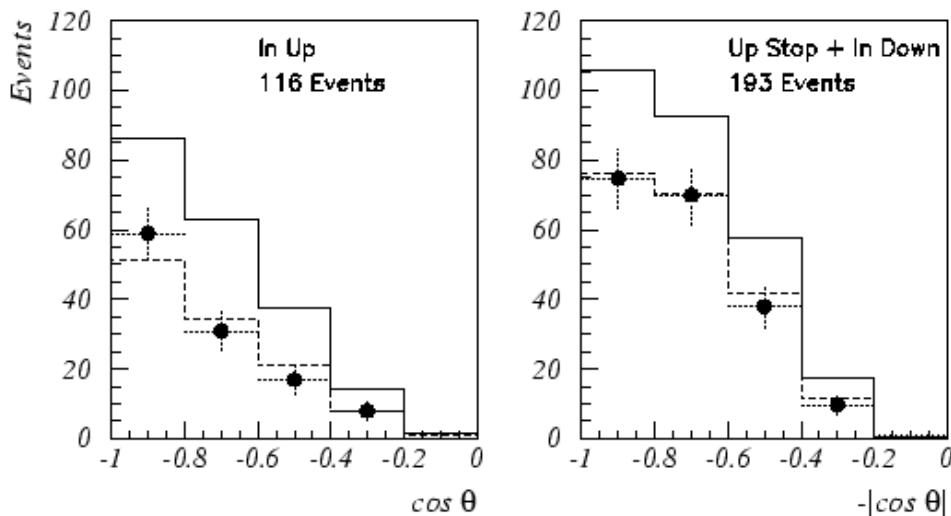


Fig. 6. Zenith angle distribution for IU (left) and US+ID events (right). The background-corrected data (black points) are compared with the Montecarlo expectation assuming no oscillation (full line) and two-flavor oscillation (dashed line) using maximum mixing and $\Delta m^2=2.5 \times 10^{-3}$ eV$^2$.

## 5. Upgoing Stopping and Internal Downgoing Muons (US+ID)

The US+ID events are identified via topological constraints, and not with the T.o.F. The main request for the event selection is the presence of one reconstructed track crossing the bottom layer of the scintillation counters. All the hits along the track must be confined at least one meter inside each wall of a MACRO supermodule. The selection conditions for the event vertex (or muon stopping point) in the detector are symmetrical to those for the IU search and reduce to a negligible level the probability that an atmospheric muon produces a background

event. The main difference with respect to the IU analysis (apart from the T.o.F.) is that on average fewer streamer tube hits are fired. To reject ambiguous and/or wrongly tracked events which passed the event selection, a visual scan was performed. All the real and simulated events which passed the event selection were randomly merged. The accepted events passed a double scan procedure (differences are included in the systematic uncertainty). Because of the lower energy of these events, the minimum range of 200 $g/cm^2$ in the apparatus is not required. Therefore the background due to upward going charged pions [13] is estimated via simulation and subtracted on statistical basis.

After the background subtraction, 193 events are classified as US+ID events.

The expected rates were evaluated with the same full Montecarlo used for IU events except for the analysis criteria. The events are mainly due to $\nu_\mu CC$, with a contribution from NC and $\nu_e$ of 13%. In absence of oscillation US events and ID events are almost equally populated. The total theoretical uncertainty on the expected rates at these energies is about 25%. The systematic error on the data, arising from the simulation of detector response and the analysis criteria is about 10%.

The expected US+ID events is 274, while the observed number of events is 193. So the ratio R of the observed number of events to the expectation becomes :

$$R = 0.71 \pm 0.05_{stat} \pm 0.07_{syst} \pm 0.18_{theor}.$$

The zenith angle distribution is shown in Fig. 7 right: it shows a uniform deficit of the measured number of events over the whole angular distribution with respect to the predictions based on the absence of neutrino oscillations.

With the neutrino oscillation parameters measured with the up-throughgoing muons ($\Delta m^2 = 0.0025$ eV$^2$ and $\sin^2 2\theta = 1$) it is expected that only US events are reduced. So the expected number of events becomes 209, well in agreement with the measured one. Moreover also the angular distribution is well in agreement with the measured one ( see dashed line in Fig. 7 right).

## 6. Ratio of IU over US+ID events

Due to the large theoretical error arising from the uncertainties on absolute $\nu$ flux and cross section, the total number of events in each category has a non negligible probability to be compatible with the no-oscillation hypothesis (6.5% for IU and 14% for US+ID events).

On the other side, using the ratio between IU and US+ID events, the theoretical error coming from neutrino flux and cross section uncertainties almost disappears. A residual 5% due to small differences between the energy spectra of the two samples survives. The systematic uncertainty on the ratio is also reduced to ~6% due to some cancellations.

The value of that ratio over the zenith angle distribution obtained from data is shown in Fig. 8, where it is compared with MC expectation.

The ratio between the total numbers of detected events is $R = 0.60 \pm 0.07_{stat}$ to be compared with $R = 0.74 \pm 0.05_{syst} \pm 0.04_{theor}$ expected in case of no oscillation.

The probability to obtain a ratio at least so far from the expected one is ~6% assuming Bartol as the true parent $\nu$ flux and taking into account the not Gaussian shape of the uncertainty on the ratio.

Taking into account oscillations, the value of R becomes 0,56, well in agreement with the measured one. Moreover also the angular distribution is well in agreement with the measured one ( see dashed line in Fig. 7 right).
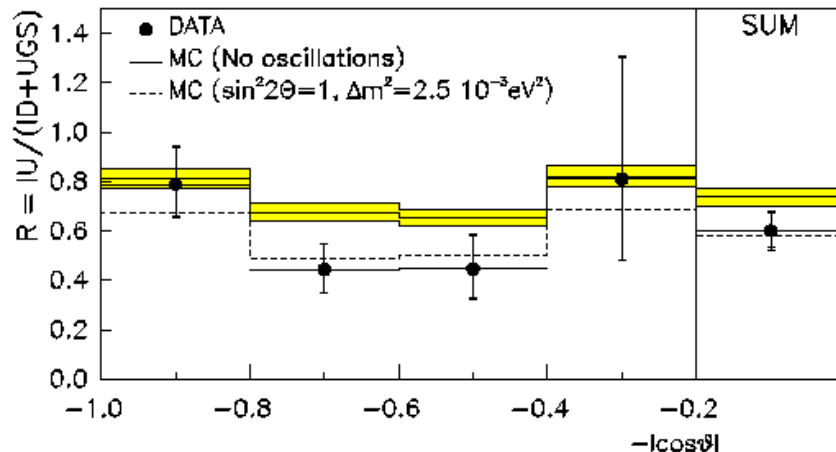
Fig. 8. Zenith angle distribution of the ratio between IU and US+ID events. The data result is compared with Montecarlo expectation assuming no oscillation (full line) and two-flavor oscillation (dashed line) using maximum mixing and $\Delta m^2 = 2.5 \times 10^{-3}$ eV$^2$.

## 7    Conclusions

The three data samples show results with a strong internal coherence in a large energy range. The results are well in agreement with the $\nu_\mu \to \nu_\tau$ oscillation hypothesis with parameters similar to those observed by Superkamiokande.

In particular, in the high energy range, the upgoing throughgoing muon data set is in favor of $\nu_\mu \to \nu_\tau$ oscillation hypothesis with a probability of 36.6% against the 0.36% for the no oscillation hypothesis ($\Delta m^2 = 0.0025$ eV$^2$ and $\sin^2 2\theta = 1$).

The results of low energy data set are also well in agreement with the oscillation hypothesis showing a large deficit for IU events and a reduced deficit for US+ID events, since only the US events ($\approx 50\%$) are expected to oscillate.

The combined statistical analysis of the three different data sets is in progress.

**References**
1)    Fukuda Y. et al., 1994, Phys. Lett. **B335**, 237.
2)    Casper D. et al. 1991, Phys. Rev. Lett. **66**, 2561.
3)    Allison W.W.M. et al., 1997, Phys. Lett. **B391**, 491.
4)    Fukuda Y. et al., 1998, Phys. Rev. Lett. **81**, 1562.
5)    Becker-Szendy R. et al., 1992, Phys. Rev. Lett. **69**, 1010.
6)    Hatakeyama S. et al., 1998, Phys. Rev. Lett. **81** 2016.
7)    Ahlen S. et al., 1995, Phys. Lett. **B357**, 481.
8)    Ambrosio M. et al., 1998, Phys. Lett. **B434**, 451.
9)    Fukuda Y. et al., 1998, hep-ex/9812014.
10)  Spurio M., 1998, Proceedings 16th ECRS, hep-ex/9808001.
11)  Bernardini P., 1998, Proceedings of "Vulcano Workshop", hep-ex/9809003.
12)  Ahlen S. et al., 1993, Nucl. Instrum. Meth. **A324**, 337.
13)  Ambrosio M. et al., 1998, Astropart. Phys. **9**, 105.
14)  Agrawal V. et al., 1996, Phys. Rev. **D53**, 1314.
15)  Glück M., Reya E. and Stratmann M., 1995, Z. Phys. **C67**, 433.
16)  Lipari P., Lusignoli M. and Sartogo F., 1995, Phys. Rev. Lett. **74**, 4384.
17)  Lohmann H., Kopp R. and Voss R., 1985, CERN-EP/85-03.
18)  Akhmedov E., Lipari P. and Lusignoli M., 1993, Phys. Lett. **B300**, 128.
19)  Liu Q.Y. and Smirnov A.Y., 1998, Nucl. Phys. **B524**, 505.